

Correlation functions and characteristic lengthscales in flat band superconductors

M. Thumin* and G. Bouzerar†

Université Grenoble Alpes, CNRS, Institut NEEL, F-38042 Grenoble, France

(Dated: 13 mai 2024)

The possibility of an unconventional form of high temperature superconductivity in flat band (FB) material does not cease to challenge our understanding of the physics in correlated systems. Recently, it has been argued that the coherence length in FB compounds could be decomposed into a conventional part of BCS type and a geometric contribution which characterises the FB eigenstates, the quantum metric. Here, we propose to address this issue in various FB systems and discuss whether the extracted characteristic lengthscales such as the size of the Cooper pairs obey this conjecture. It is found that the relevant lengthscales are less than one lattice spacing, weakly sensitive to the strength of the electron-electron interaction, and more importantly disconnected from the quantum metric.

INTRODUCTION

Over the past ten years we are witnessing a rapidly growing interest for the physics in dispersion-less bands [1–8]. In flat band (FB) compounds, because the width of these bands is extremely narrow, the Coulomb energy is left as the unique relevant energy scale. This places naturally these systems in the class of highly correlated materials and opens the access to exotic and unexpected physical phenomena and quantum phases. Undeniably, one of the most striking feature is the possibility of high critical temperature superconductivity (SC) in compounds where the Fermi velocity vanishes [9–18]. This unconventional form of SC is of inter-band nature and characterised by a geometrical quantity known as the quantum metric (QM). The QM is connected to the real part of the quantum geometric tensor [19, 20] and provides a measure of the typical surface associated to the FB Bloch eigenstates. So far, the unique experimental realisation of such an unusual form of superconductivity is very likely the one that has been observed in twisted bilayer of graphene (Moiré) in the vicinity of magic angles [8, 21–26].

It is well known that in conventional BCS systems where the SC is of intra-band nature [27, 28], the coherence length ξ_c is given by $\xi_{BCS} = \frac{\hbar v_F}{\Delta}$ where v_F and Δ are respectively the Fermi velocity and superconducting gap or pairing amplitude. We recall that ξ_c measures the size of the Cooper pair in real space. Since, in the BCS regime (weak coupling) the SC gap is exponentially small, ξ_c is often extremely large, hence Cooper pairs are highly overlapping with each other. On the other hand, in the strong coupling regime the Cooper pairs can be assimilated to tightly bound non-overlapping composite bosons which at low temperature leads to the well known Bose Einstein condensation phenomenon (BEC)[29, 30].

A natural question arises : what about the case of FB superconductors? Recently, it has been argued that the coherence length in these systems has two contributions, the first is of conventional type and the other is purely geometric in nature [31, 32]. More precisely, it is

claimed that the coherence length can be expressed as $\xi_c = \sqrt{\xi_{BCS}^2 + \langle g \rangle}$ where $\langle g \rangle$ is the average of the QM. Hence, if the band is rigorously flat the first term vanishes.

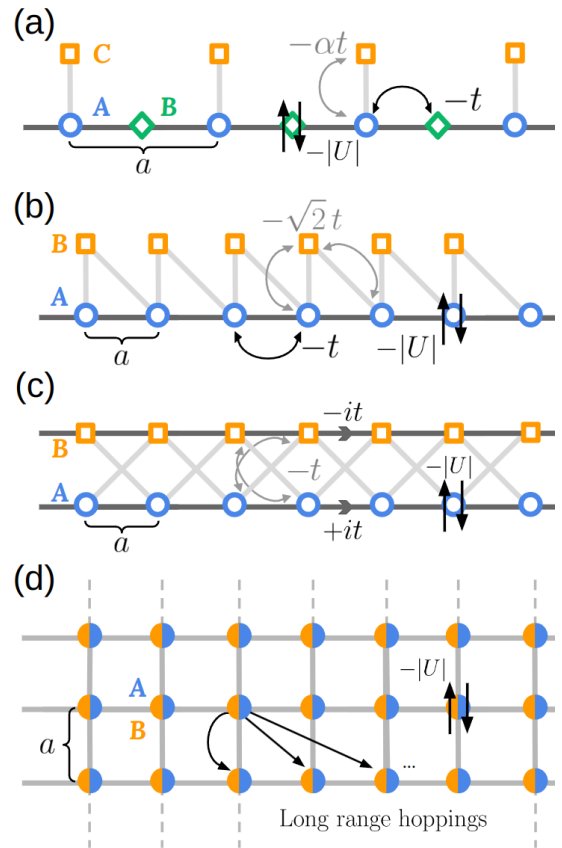


FIGURE 1. Schematic representation of (a) the stub lattice (StL), (b) the sawtooth chain (SaL), (c) the Creutz ladder (CrL) and (d) the two-dimensional χ -lattice (χ -L). The hoppings and the on-site Hubbard attractive interaction term are depicted in the figure. In the case of the χ -L (two orbitals A and B per site) the hoppings are long range (see main text).

The purpose of the present study is to address this issue in several FB lattices and discuss our findings in

connection with these predictions and with the existing literature. More precisely, we propose to consider four different systems, three of them are one dimensional and the last one is two dimensional : the stub lattice (StL), the sawtooth chain (SaL), the Creutz ladder (CrL) and the χ -lattice (χ -L). These models are illustrated in Fig.1. Notice that the χ -L has been originally introduced in Ref. [33]. However, since no specific name has been attributed to this peculiar model, " χ -lattice" has been chosen. In this system, the range of the extended hoppings is controlled by a single parameter (χ) as it will become more explicit in the next paragraph. The choice of these four different systems is motivated by several intentions. It allows to estimate the impact of (i) the bipartite character of the lattice, (ii) the tunability of the quantum metric, (iii) the absence of dispersive bands in the spectrum, (iv) and last the lattice dimension.

THEORY AND METHODS

Electrons are described by the attractive Hubbard model which reads,

$$\hat{H} = \sum_{i\lambda, j\eta, \sigma} t_{ij}^{\lambda\eta} \hat{c}_{i\lambda, \sigma}^\dagger \hat{c}_{j\eta, \sigma} - \mu \hat{N} - |U| \sum_{i\lambda} \hat{n}_{i\lambda, \uparrow} \hat{n}_{i\lambda, \downarrow}, \quad (1)$$

where $\hat{c}_{i\lambda, \sigma}^\dagger$ creates an electron of spin σ at site $\mathbf{r}_{i\lambda}$, i being the cell index and λ the orbital index ranging from 1 to n_{orb} . $\hat{N} = \sum_{i\lambda, \sigma} \hat{n}_{i\lambda, \sigma}$, μ is the chemical potential and $|U|$ is the strength of the on-site attractive electron-electron interaction. The hoppings are very short ranged in StL, SaL and CrL as depicted in Fig.1. On the other hand, in the χ -L the situation differs, the hoppings are long-ranged, restricted to (A, B) -pairs, and given by $t_{ij}^{AB} = -\frac{t}{N_c} \sum_{\mathbf{k}} e^{i\mathbf{k}\cdot\mathbf{r}} e^{i\alpha_{\mathbf{k}}}$ where $\alpha_{\mathbf{k}} = \chi(\cos(k_x a) + \cos(k_y a))$, $\mathbf{r} = \mathbf{r}_j - \mathbf{r}_i$, and N_c being the number of unit cells. The parameter χ controls both the range of the hoppings and the QM which is given by $\langle g \rangle = \chi^2 a^2 / 8$ [34].

In this work, we treat the interaction term within the Bogoliubov de Gennes (BdG) approach which consists in the following decoupling scheme,

$$\begin{aligned} \hat{n}_{i\lambda, \uparrow} \hat{n}_{i\lambda, \downarrow} &\stackrel{BdG}{\simeq} \langle \hat{n}_{i\lambda, \downarrow} \rangle \hat{n}_{i\lambda, \uparrow} + \langle \hat{n}_{i\lambda, \uparrow} \rangle \hat{n}_{i\lambda, \downarrow} \\ &+ \frac{\Delta_{i\lambda}}{|U|} \hat{c}_{i\lambda, \uparrow}^\dagger \hat{c}_{i\lambda, \downarrow}^\dagger + \frac{\Delta_{i\lambda}^*}{|U|} \hat{c}_{i\lambda, \downarrow} \hat{c}_{i\lambda, \uparrow}, \end{aligned} \quad (2)$$

where the self-consistent parameters $\langle \hat{n}_{i\lambda, \sigma} \rangle$ and $\Delta_{i\lambda} = -|U| \langle \hat{c}_{i\lambda, \downarrow} \hat{c}_{i\lambda, \uparrow} \rangle$ are respectively the orbital dependent occupations and pairings. $\langle \dots \rangle$ corresponds to the grand canonical average. Notice, that the total carrier density is defined as $n = N_e / N_c$, where N_e is the total number of electrons, hence n varies from 0 to $2n_{orb}$.

Before we discuss our calculations, we propose to provide some arguments that justify that our approach is meaningful. We first start with the shortcomings. It is

well established that the BdG Hamiltonian being quadratic, it is inappropriate to calculate reliably two particles correlation functions (CFs) such as the pairing-pairing correlation function $f_P(\mathbf{r}_i - \mathbf{r}_j) = \langle \hat{\Pi}_i^\dagger \hat{\Pi}_j \rangle$ where the on-site pairing operator (s-wave) $\hat{\Pi}_i^\dagger = \hat{c}_{i\uparrow}^\dagger \hat{c}_{i\downarrow}^\dagger$. In the case of the attractive Hubbard model in two dimensional systems, one expects the correlation function $f_P(\mathbf{r})$ to decay algebraically with a T -dependent power for $T < T_{BKT}$, and exponentially when $T > T_{BKT}$, where T_{BKT} is the Berezinskii-Kosterlitz-Thouless transition temperature [35–37]. On the other hand, the one-particle CF of the form $f_{sp}^\sigma(\mathbf{r}_i - \mathbf{r}_j) = \langle \hat{c}_{i\sigma}^\dagger \hat{c}_{j\sigma} \rangle$ always decays exponentially both in the superconducting phase and in the normal phase. Mean Field theory such as the BdG approach can not describe the change of behaviour of $f_P(\mathbf{r})$ across the BKT transition, since through Wick's theorem two-particles CFs reduce to products of one-particle CFs only. However, in FB systems, one expects the single particle CFs to be well captured within the BdG theory. For instance, it has been shown, that the local occupations, the pairings and the superfluid weight calculated by the numerically unbiased DMRG are in excellent agreement with the mean field values in the CrL and in the SaL [12, 38]. It should be emphasised that the agreement found concerns both the weak and the strong coupling regime. In what follows it will be shown that it is as well the case for correlations functions.

To study the characteristic lengthscales in the SC phase at $T = 0$, we define the normal and anomalous CFs,

$$G_{\alpha\beta}(\mathbf{r}) = \langle \hat{c}_{i\alpha, \sigma}^\dagger \hat{c}_{j\beta, \sigma} \rangle, \quad (3)$$

$$K_{\alpha\beta}(\mathbf{r}) = \langle \hat{c}_{i\alpha, \uparrow} \hat{c}_{j\beta, \downarrow} \rangle, \quad (4)$$

where the index i (respectively j) refers to the unit cell position \mathbf{r}_i (respectively \mathbf{r}_j), α (resp. β) labels the orbitals and $\mathbf{r} = \mathbf{r}_j - \mathbf{r}_i$. Here, the spin index $\sigma = \uparrow, \downarrow$ is irrelevant, the SC phase being non magnetic. The CF $K_{\alpha\beta}$ is particularly of interest since it allows the extraction of the Cooper pair size. Indeed, in the case of a single one dimensional dispersive band problem (conventional SC) it can be shown analytically that $K_{\alpha\alpha}(\mathbf{r}) \simeq \frac{1}{\sqrt{|\mathbf{r}|}} e^{-|\mathbf{r}|/\xi_{BCS}}$ for $|\mathbf{r}| \rightarrow \infty$ as addressed in the next paragraph.

RESULTS AND DISCUSSIONS

Coherence length in dispersive bands

Before we discuss in details the case where the Fermi energy coincides with that of the FB, it is interesting to analyse the situation where it is located inside the dispersive bands. To illustrate this scenario, we consider the quarter filled SaL. This density corresponds to the half-filling of the lower dispersive band.

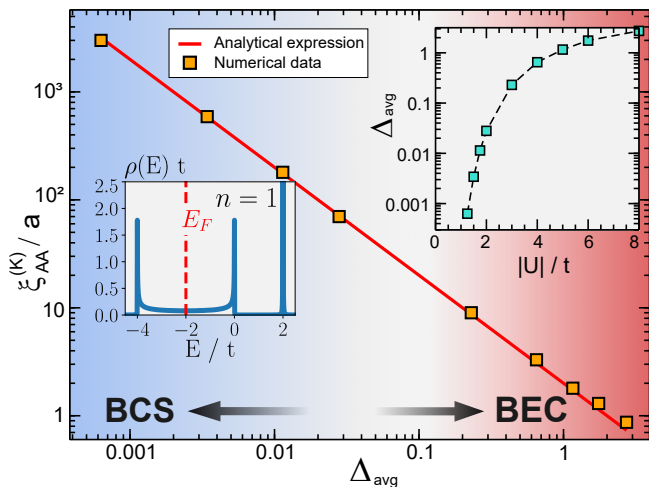


FIGURE 2. $\xi_{AA}^{(K)}$ as a function of the averaged pairing Δ_{avg} in the quarter filled sawtooth chain (SaL). The red thick line is the BCS formula $\frac{\hbar v_F}{\Delta_{avg}}$ where $\hbar v_F = 2at$. The first inset (top right) shows the correspondence between $|U|$ and Δ_{avg} and the other one illustrates the density of states for $|U| = 0$, with $E_F = -2t$ for the quarter filling. The BCS regime corresponds to $\xi_{AA}^{(K)} \gg a$ and BEC to $\xi_{AA}^{(K)} \leq a$.

In Fig.2, $\xi_{AA}^{(K)}$ is plotted as a function of the averaged pairing Δ_{avg} in the quarter filled SaL where $\Delta_{avg} = \frac{1}{2}(\Delta_A + \Delta_B)$ (A and B sites are inequivalent). This characteristic lengthscale is obtained from a fit of the form $\frac{1}{\sqrt{|\mathbf{r}|}} e^{-|\mathbf{r}|/\xi_{AA}^{(K)}}$ of the long distance behaviour of the anomalous CF $K_{AA}(\mathbf{r})$. The BCS-like expression (red thick line in the figure) is defined as $\frac{\hbar v_F}{\Delta_{avg}}$. Here the Fermi velocity $v_F = \frac{2at}{\hbar} \sin(k_F a)$ where $k_F a = \frac{\pi}{2}$ for the quarter filled SaL. It is striking to see that the excellent agreement found between the numerical data and the BCS expression is not restricted to the weak coupling regime ($\Delta_{avg} \ll t$). Indeed, remarkably the agreement is obtained for values of the average pairing that varies over four decades (see inset of Fig.2), which corresponds to $|U|/t$ that varies from 1 to 8.

The case of half-filled bipartite lattices

We consider the specific case of half-filled bipartite lattices where the number of orbitals in one sublattice is larger than that of the other, implying that at least one FB is located at $E = 0$. We propose to demonstrate the following remarkable property, valid for any $|U|$,

$$G_{\lambda\lambda}(\mathbf{r}) = \frac{1}{2}\delta(\mathbf{r}). \quad (5)$$

In a recent study [39] it has been shown that the Bogoliubov quasi-particle (QP) eigenstates present an interesting symmetry in half-filled systems. If \mathcal{A} (resp. \mathcal{B}) denotes

the first (resp. second) sublattice which contain Λ_A (resp. Λ_B) orbitals per unit cell, the QP eigenstates can be subdivided in two families \mathcal{S}^+ and \mathcal{S}^- defined in what follows. First, a generic QP eigenstate (in momentum space) has the form $|\Psi\rangle = (|\Psi^\uparrow\rangle, |\Psi^\downarrow\rangle)^t$ where the first Λ_A (resp. next Λ_B) rows of $|\Psi^\sigma\rangle$ are the components on sublattice \mathcal{A} (resp. \mathcal{B}). This eigenstate belongs to the subspace \mathcal{S}^+ (resp. \mathcal{S}^-) if $|\Psi^\downarrow\rangle = \hat{M}|\Psi^\uparrow\rangle$ (resp. $|\Psi^\downarrow\rangle = -\hat{M}|\Psi^\uparrow\rangle$) where the matrix $\hat{M} = \text{diag}(\hat{1}_{\Lambda_A}, -\hat{1}_{\Lambda_B})$. Additionally, for any finite $|U|$, it has been shown in Ref. [39] that the subset \mathcal{S}^- (respectively \mathcal{S}^+) consists exactly in Λ_B (respectively Λ_A) eigenstates of positive or zero energy and Λ_A (respectively Λ_B) eigenstates of strictly negative energy.

Now, start with the definition $G_{\lambda\lambda}(\mathbf{r}) = \frac{1}{N_c} \sum_{\mathbf{k}} e^{i\mathbf{k}\cdot\mathbf{r}} \langle \hat{O}_{\lambda\mathbf{k},\uparrow} \rangle$ where $\hat{O}_{\lambda\mathbf{k},\uparrow} = c_{\mathbf{k}\lambda,\uparrow}^\dagger c_{\mathbf{k}\lambda,\uparrow}$. At $T = 0$, its grand canonical average is given by,

$$\langle \hat{O}_{\lambda\mathbf{k},\uparrow} \rangle = \sum_m \langle \Psi_{m\mathbf{k}}^< | \hat{O}_{\lambda\mathbf{k},\uparrow} | \Psi_{m\mathbf{k}}^< \rangle, \quad (6)$$

where $|\Psi_{m\mathbf{k}}^< \rangle$ are the QP eigenstates of the BdG Hamiltonian of negative energy, m being band index. Using the closure relation, $\sum_{m,s=<, >} |\Psi_{m\mathbf{k}}^s\rangle \langle \Psi_{m\mathbf{k}}^s| = 1$, where the sum runs over QP eigenstates with positive ($s = >$) and negative energy ($s = <$) and the symmetry mentioned above one can show that,

$$\sum_m \langle \Psi_{m\mathbf{k}}^< | \hat{O}_{\lambda\mathbf{k},\uparrow} | \Psi_{m\mathbf{k}}^< \rangle = \sum_m \langle \Psi_{m\mathbf{k}}^> | \hat{O}_{\lambda\mathbf{k},\uparrow} | \Psi_{m\mathbf{k}}^> \rangle, \quad (7)$$

which combined with Eq.(6) leads to $\langle \hat{O}_{\lambda\mathbf{k},\uparrow} \rangle = \frac{1}{2}$ and demonstrates Eq.(5).

It is interesting to remark that our proof can be straightforwardly extended to the case of disordered systems that preserve the bipartite character of the lattice, such as the presence of vacancies or bond disorder.

The Stub lattice

The StL is bipartite and offers the possibility to tune the QM without changing the nature of the compact localized eigenstates. The QM is controlled by the A-C hopping (αt) (see Fig.1) and given by $\langle g \rangle = \frac{1}{2|\alpha|\sqrt{2+\alpha^2}}$ [40]. The StL has been studied in great details in Refs. [18, 41]. Here, we restrict our study to the case $\alpha = 0.5$ and $n = 3$ which corresponds to a half-filled FB with $\langle g \rangle \simeq 0.7$.

First, one can already conclude from the previous section that the conventional CFs ($G_{\alpha\alpha}$) are given by Eq.(5), which is indeed what we find numerically for any $|U|$ and any α . Figure 3(a) depicts the anomalous CF K_{CC} as a function of $|\mathbf{r}|$ for several values of $|U|$ which correspond to weak, intermediate and strong coupling regime. As it can be clearly seen, in all cases this CF decays exponentially with a lengthscale $\xi_{CC}^{(K)}$ (Cooper pair size)

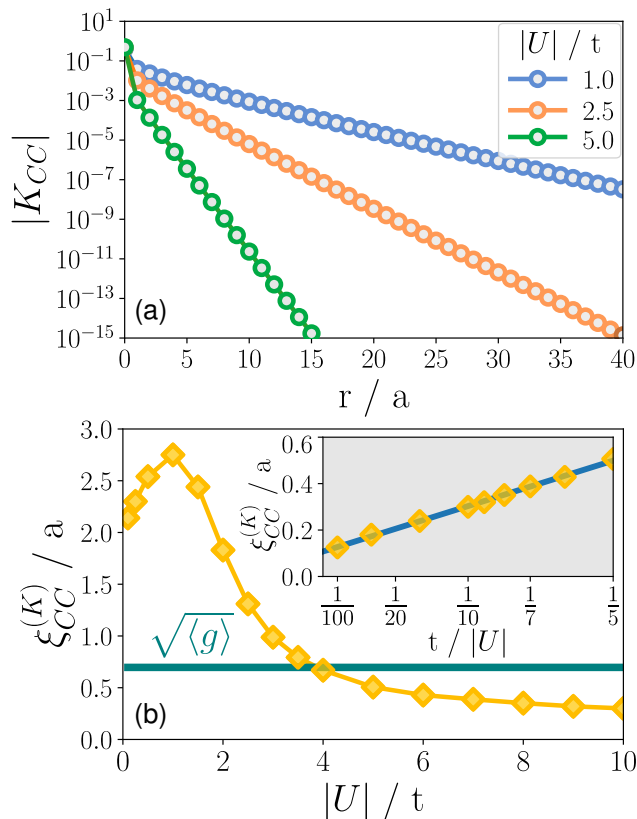


FIGURE 3. (a) K_{CC} as a function of r in the stub lattice (StL) for several values of $|U|/t$ (1, 2.5 and 5). (b) $\xi_{CC}^{(K)}$ as a function of $|U|$. The (dark-green) horizontal line depicts the square root of the quantum metric $\langle g \rangle$. The inset shows $\xi_{CC}^{(K)}$ for $|U| \gg t$. Here, α is set to 0.5 (see Fig.1) and the carrier density is fixed to $n = 3$ which corresponds to half-filling.

that reduces rapidly as $|U|$ increases. The variation of the extracted lengthscale $\xi_{CC}^{(K)}$ is plotted as a function of $|U|/t$ in Fig.3(b). In the limit of vanishing $|U|/t$ it is approximately (for this value of α) $2a$, then it increases and reaches a maximum for $|U|/t = 1.5$ and beyond it decreases continuously. There is no simple explanation for the origin of this maximum, since for larger values of α it disappears. The inset represents, its behaviour in the large $|U|/t$ limit. It is found that $\xi_{CC}^{(K)} \rightarrow 0.125a$. As it can be seen, $\xi_{CC}^{(K)}$ crosses $\sqrt{\langle g \rangle} = 0.7a$ at $|U|/t \approx 4$ and converges to a much smaller value. The large $|U|/t$ behaviour, is consistent with the fact that in the BEC regime, the Cooper pair size is expected to be very small. Remark that K_{BB} and K_{AA} vary similarly with the same lengthscale.

The sawtooth chain

In contrast to the StL, the SaL as illustrated in Fig.1(b), is a non bipartite lattice and does not allow

the tuning of the QM. The FB exists only when the AB-hoppings (1st and 2nd neighbours) are $-\sqrt{2}t$. The superconductivity in the StL has been addressed in details in Ref. [38] using a numerically exact method : the DMRG. It has been shown that the BdG approach reproduces accurately the exact results, for both the pairings and the superfluid weight. In Fig.4(a), both G_{AA} and K_{AA} are plotted as a function of $|\mathbf{r}|$, for different values of $|U|$. Here, the electron density is set to $n = 3$ which corresponds to the half-filled FB. As it can be seen, the lengthscales associated to the decay of G_{AA} and K_{AA} are almost identical both in the weak and strong coupling regime. Additionally, the slope appears to vary weakly. Notice that G_{BB} and K_{BB} behave similarly. Fig.4(b) depicts the variation of $\xi_{AA}^{(K)}$ as a function of $t/|U|$. The inset describes the weak coupling regime. In this regime, $\xi_{AA}^{(K)} \approx 0.735a$ and almost insensitive to $|U|$. As $|U|$ increases further, $\xi_{AA}^{(K)}$ decays monotonously. As seen in the case of the StL, $\xi_{AA}^{(K)}$ crosses $\sqrt{\langle g \rangle}$ when $t/|U| \approx 0.05$ and converges towards $0.2a$. In the SaL, it can be shown that the minimal QM is $\langle g \rangle = \frac{1}{4\sqrt{3}}$. We should mention as well that our values of $G_{AA}(r)$ are consistent with the DMRG calculations of Ref. [38].

The Creutz ladder

The CrL depicted in Fig1(c) is particularly interesting since its dispersion consists only in FBs, located at $E = \pm 2t$ in the non-interacting case. As a consequence of the uniform pairings, these bands remain flat when $|U|$ is non-zero. The superconductivity in the CrL have been addressed exactly, within the DMRG approach in Refs [12, 38]. As in the case of the sawtooth chain, it has been revealed that pairings and superfluid weight are accurately captured by the BdG theory. The A and B sites being equivalent, we focus our attention on $|K_{AA}|$ and $|G_{AA}|$. In addition, we consider the case of the quarter filled ladder (half-filled lower FB) which corresponds to $n = 1$. Both CFs are plotted in Fig.5 as a function of $|\mathbf{r}|$ for several values of $|U|$ ranging from weak to strong coupling regime. As it can be seen these two CFS behave similarly. Surprisingly, it is found that there are only two non-vanishing values corresponding respectively to $|\mathbf{r}| = 0$ and a . For larger distances, $|K_{AA}|$ and $|G_{AA}|$ are zero within the numerical accuracy. This is illustrated in the inset of Fig.5(b) where for $|\mathbf{r}| = 2a$ the CF $|G_{AA}|$ drops by 16 orders of magnitude. It is found as well that $|K_{AA}|(|\mathbf{r}| = a)$ decays very rapidly as $|U| \geq 1$ and eventually vanishes when $|U| \rightarrow \infty$. Thus, the Cooper pair size varies between 1 and 0 where 0 corresponds to $|U| = \infty$.

In the Appendix A, we demonstrate analytically in the

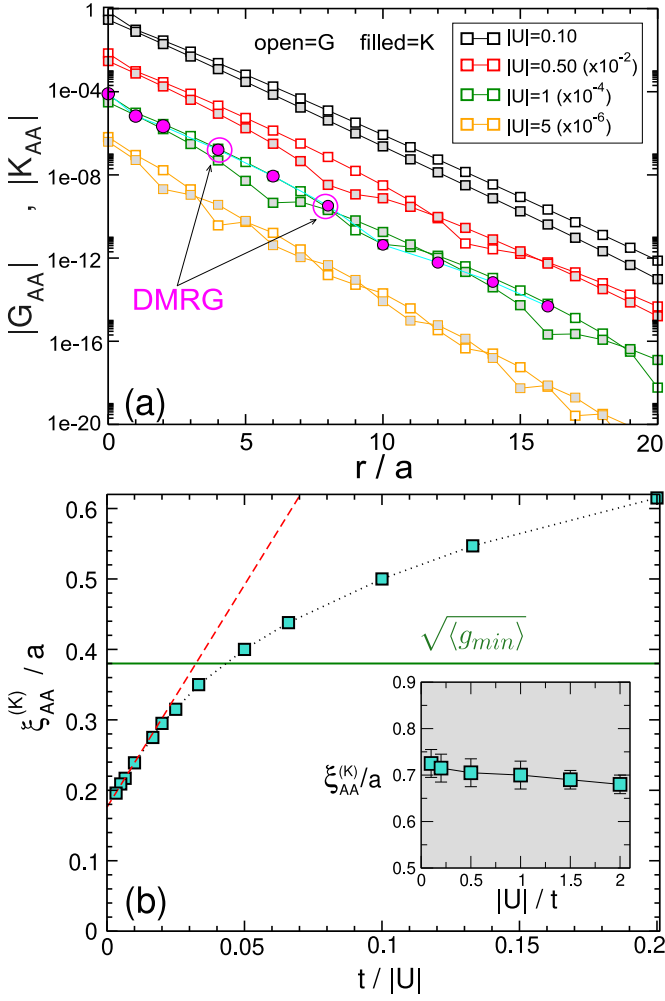


FIGURE 4. (a) $|G_{AA}|$ and $|K_{AA}|$ as a function of r in the sawtooth chain (SaL) for several values of $|U|$. For the sake of clarity, $|G_{AA}|$ and $|K_{AA}|$ have been multiplied by 10^{-2} , 10^{-4} and 10^{-6} for $|U| = 0.5, 1$ and 5 respectively. The carrier density is $n = 3$ (half-filled FB). DMRG data for $|U| = 1$ from Ref. [38] are shown as well. (b) $\xi_{AA}^{(K)}/a$ as a function of $t/|U|$. The horizontal lines depicts the square root of the minimal quantum metric $\langle g_{min} \rangle$. The inset represents $\xi_{AA}^{(K)}/a$ as a function of $|U|$ for small values of $|U|$. The dashed red line is a linear fit for $\frac{t}{|U|} \leq 0.03$.

case of weak coupling that the CFs are given by,

$$\begin{aligned} G_{AA}(r) = K_{AA}(r) &= \frac{1}{4}\delta_{r,0} - \frac{i}{8}\delta_{r,a} + \frac{i}{8}\delta_{r,-a}, \\ G_{AB}(r) = K_{AB}(r) &= \frac{1}{8}(\delta_{r,a} + \delta_{r,-a}). \end{aligned} \quad (8)$$

We point out the fact that the analytic expression found for $G_{AA}(r)$ is consistent with the exact results obtained from DMRG calculations [12]. Indeed, it has been found (see Fig.10 in this manuscript) that for $r \geq 2a$, $G_{AA} \leq 10^{-12}$.

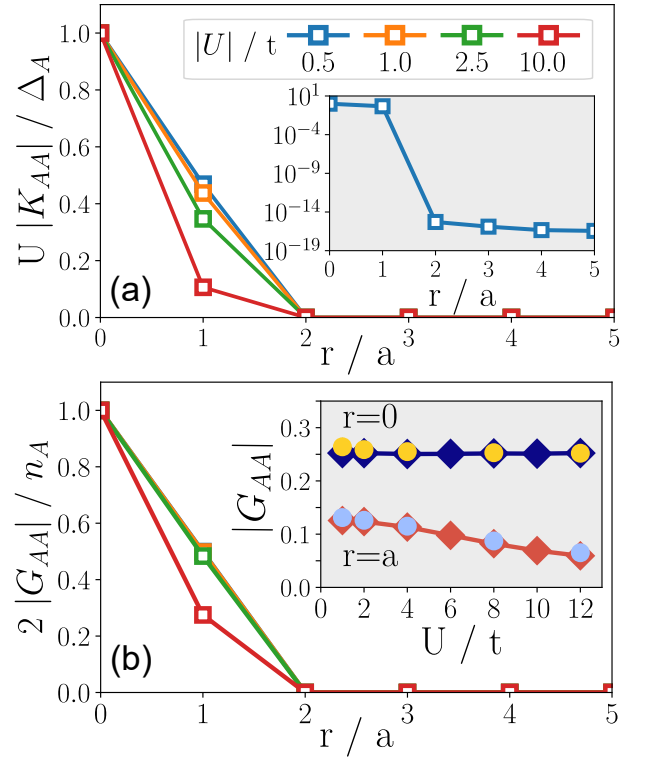


FIGURE 5. (a) $|K_{AA}|$ and (b) $|G_{AA}|$ as a function of r in the Creutz ladder (CrL) for several values of $|U|$. The charge density is fixed $n = 1$. For $r \geq 2a$, both $|K_{AA}|$ and $|G_{AA}|$ are zero within our numerical precision. The inset in (a) represents $|K_{AA}|$ in log scale. The inset in (b) shows $|G_{AA}|$ as a function of $|U|$ for $r = 0$ and $r = a$. Diamonds are our calculations and circles are the DMRG data of Ref. [12]

The χ -Lattice

The χ -L is a two dimensional system in which both electronic bands are dispersion-less and located at $E = \pm t$. As mentioned earlier this system has been introduced originally in Ref. [33]. The superconductivity has been addressed within the Quantum Monte Carlo (QMC) method in Ref. [34] and within a mean field approach in Ref. [32]. We recall that the dimensionless parameter χ controls both the range of the hoppings and the value of the QM. Here, we focus on the quarter filled system which corresponds to a charge density $n = 1$. As it is the case in the CrL, the orbitals A and B are equivalent, pairings are identical on both sites. In addition, because the long range hoppings connects A to B sites only, this lattice is bipartite as well.

Let us now discuss our results. First, for any value of both $|U|$ and χ , with high numerical accuracy we find,

$$\frac{4}{n}G_{\alpha\alpha}(\mathbf{r}) = \frac{|U|}{\Delta}K_{\alpha\alpha}(\mathbf{r}) = \delta(\mathbf{r}), \quad (9)$$

where $\alpha = A, B$. These features are illustrated in Fig.6 (a) and (b). It should be emphasised that the pro-

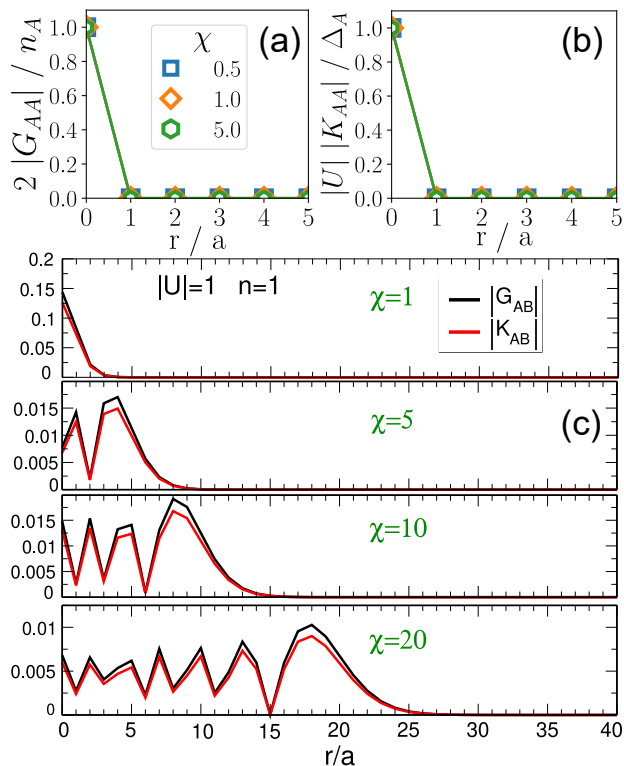


FIGURE 6. (a) and (b) $|G_{AA}|$ and $|K_{AA}|$ as a function of r (along the x -direction) in the χ -L for several values of χ . (c) same as in (a) and (b) for the off-diagonal correlation functions $|G_{AB}|$ and $|K_{AB}|$. The carrier density is $n = 1$ and the Hubbard parameter $|U| = 1$.

perty given in Eq.(5) concerns only the case of half-filled bipartite lattices. Here, our system is quarter filled, which means that our findings are specific to the χ -L. As a consequence, for any $|U|$ the Cooper pair size is zero. In the Appendix B, we have demonstrated analytically Eq.(9) in the weak coupling regime.

More strikingly, we have found that the off-diagonal correlation functions $|G_{AB}|$ and $|K_{AB}|$ exhibit an unexpected behaviour as it can be clearly seen in Fig.6(c). First, one finds that $|G_{AB}|$ and $|K_{AB}|$ are very similar for any value of χ . Furthermore, for a given χ , one can distinguish two distinct regimes. First, for $|\mathbf{r}| \leq \chi a$ the CFs oscillates as $|\mathbf{r}|$ increases. Secondly, when $|\mathbf{r}| \geq \chi a$ it decays monotonously as the distance increases. However, any attempt to fit the tail by a function of the form $r^{-\alpha} e^{-|\mathbf{r}|/\beta}$ is unsuccessful. Hence, one cannot extract any characteristic lengthscale from these off-diagonal correlation functions. In the Appendix B, we have calculated analytically the G_{AB} and K_{AB} as a function of \mathbf{r} in the limit of small values $|U|$. It is shown that $G_{AB}(\mathbf{r}) = K_{AB}(\mathbf{r}) = \frac{1}{4N_c} \sum_{\mathbf{k}} e^{i\mathbf{k}\cdot\mathbf{r}} e^{-i\alpha\mathbf{k}}$. This means that for this specific lattice the off-diagonal CFs coincides up to a coefficient with the (A,B) hoppings in real-space. In addition, in the limit of large $|\mathbf{r}|$ along the x -direction, it is

shown that,

$$G_{AB}(\mathbf{r}) \propto (-i)^{n_x} J_0(\chi) \frac{1}{\sqrt{2\pi n_x}} e^{n_x \cdot \ln(\frac{e\chi}{2n_x})}, \quad (10)$$

where $\mathbf{r} = (n_x a, 0)$ and J_0 is the Bessel function of the first kind and order 0. This clarifies why we could not extract a typical lengthscale from the numerical data plotted in Fig.6(c).

Connection with recent studies

In this paragraph, we would like to discuss the connection between our findings and recent studies [31, 32]. It is claimed in these articles, that the coherence length in quasi FBs can be expressed as, $\xi_c = \sqrt{\xi_{BCS}^2 + \langle g \rangle}$ where $\langle g \rangle$ is the average of the quantum metric (minimal). The BCS contribution vanishes when the band is rigorously flat. In Ref. [32], the authors have illustrated their point by considering the χ -L. Based on the fact that the coherence length is extracted from the long distance decay of $K_{\alpha\alpha}$ our findings clearly contradicts their prediction. Indeed, in the specific case of the χ -L we have found that for any $|U|$ and any χ , thus any QM, the size of the Cooper pair is always zero. What is the origin of this contradiction? In Ref. [32], the authors have treated the electron-electron correlation at the mean field level, similar to ours. However, their decoupling of the Hubbard term is performed in momentum space instead of real space as done within the BdG approach. Additionally, the authors have performed a projection of the fermionic operators onto the lowest FB which is, in their work, the key step so that the QM can emerge. In contrast, in our BdG approach we perform no projection and treat essentially the electron-electron correlation at the same level, thus it is striking that our results differ from those of Ref. [32]. This may suggest that the origin of the disagreement could be the projection procedure. Notice that, in their work, the authors have considered the pair-pair correlation function of the form, $C_{\alpha\beta}(\mathbf{r}) = \langle \hat{c}_{i\alpha\uparrow}^\dagger \hat{c}_{i\beta\downarrow}^\dagger \hat{c}_{0\beta\downarrow} \hat{c}_{0\alpha\uparrow} \rangle$ which within mean field reduces to, $C_{\alpha\beta}(\mathbf{r}) \xrightarrow{MF} G_{\alpha\alpha}(\mathbf{r}) G_{\beta\beta}(\mathbf{r}) + |K_{\alpha\beta}(\mathbf{0})|^2$. Thus, our conclusion does not change, since the diagonal CFs $G_{\alpha\alpha}(\mathbf{r})$ ($\alpha = A, B$) reduce to δ -functions as given in Eq.(9).

CONCLUSION

To conclude, we have investigated the normal and anomalous correlations in various flat band systems and extracted the associated characteristic lengthscales. It is found that the size of the Cooper pairs is less than one lattice spacing, both in the weak and strong coupling regime. We have shown as well that the normal correlation function reduces to a Dirac function in the case of

half-filled bipartite lattices. Finally, in contrast with a recent claim it appears that the coherence length is disconnected from the quantum metric.

ACKNOWLEDGEMENT

We thank George Batrouni, Si Min Chan and Benoit Grémaud for kindly sending us their DMRG data.

APPENDIX A : THE CORRELATION FUNCTIONS IN THE CREUTZ LADDER

In this appendix we propose to derive analytically the correlations functions G and K as defined in the main text in the quarter filled Creutz ladder. We focus our attention on small values of $|U|$. We restrict our calculation to $T = 0$. The BdG Hamiltonian reads,

$$\hat{H}_{BdG} = \sum_k \hat{\Psi}_k^\dagger \begin{pmatrix} \hat{h}_k^\uparrow & \Delta \hat{1}_{2 \times 2} \\ \Delta^* \hat{1}_{2 \times 2} & -\hat{h}_k^{\downarrow*} \end{pmatrix} \hat{\Psi}_k, \quad (\text{A.1})$$

where we have introduced the Nambu spinor $\hat{\Psi}_k^\dagger = (\hat{c}_{Ak\uparrow}, \hat{c}_{Bk\uparrow}, \hat{c}_{A-k\downarrow}, \hat{c}_{B-k\downarrow})^t$ and the block matrix,

$$\hat{h}_k^\uparrow = \begin{pmatrix} -2t \sin(ka) - \tilde{\mu} & -2t \cos(ka) \\ -2t \cos(ka) & 2t \sin(ka) - \tilde{\mu} \end{pmatrix}, \quad (\text{A.2})$$

where we have introduced $\tilde{\mu} = \mu + \frac{|U|}{4}n$. Because of time reversal symmetry $\hat{h}_k^{\downarrow*} = \hat{h}_k^\uparrow$. Notice as well that the pairing Δ , uniform because A and B sites are equivalent, can be taken real. Here, the total carrier density $n = 2n_A = 2n_B$ is set to 1.

First, we consider the case $|U| = 0$ for which the chemical potential $\mu = \mu_0 = -2t$. The quasi-particle (QP) eigenvalues are $E_{1,4} = \pm 4t$, and $E_{2,3} = 0$ which is doubly degenerate. The corresponding QP eigenstates are of the form, $|\Psi_i\rangle = (|\psi_i^\uparrow\rangle, |\psi_i^\downarrow\rangle)^t$, where $i = 1, \dots, 4$. More precisely they are given by, $|\Psi_1^0\rangle = (0, |\phi_0^+\rangle)^t$, $|\Psi_2^0\rangle = (|\phi_0^-\rangle, 0)^t$, $|\Psi_3^0\rangle = (0, |\phi_0^-\rangle)^t$, and $|\Psi_4^0\rangle = (|\phi_0^+\rangle, 0)^t$, where,

$$|\phi_0^\pm\rangle = \frac{1}{\sqrt{2}} \frac{1}{\sqrt{1 \pm \sin(ka)}} \begin{pmatrix} -\cos(ka) \\ \sin(ka) \pm 1 \end{pmatrix}. \quad (\text{A.3})$$

When the Hubbard term is switched on, we apply a perturbation theory for degenerate pair eigenstates ($|\Psi_2^0\rangle, |\Psi_3^0\rangle$) that leads to, $E_\pm = \pm \sqrt{(\delta\tilde{\mu})^2 + \Delta^2}$ where $\delta\tilde{\mu} = \tilde{\mu} - \mu_0$. The corresponding QP eigenstates are,

$$|\Psi_\pm\rangle = \frac{1}{\sqrt{N^\pm}} \left(\Delta |\Psi_2^0\rangle + (\delta\tilde{\mu} \pm \sqrt{(\delta\tilde{\mu})^2 + \Delta^2}) |\Psi_3^0\rangle \right), \quad (\text{A.4})$$

where $N^\pm = 2 \left(\delta\tilde{\mu}^2 + \Delta^2 \pm \delta\tilde{\mu} \sqrt{(\delta\tilde{\mu})^2 + \Delta^2} \right)$.

Using the self-consistent equations for the carrier density

which for each spin sector is $1/4$ and the gap equation one finds in the limit of small $|U|$,

$$\delta\tilde{\mu} = 0 + o(|U|^2), \quad (\text{A.5})$$

$$\Delta = \frac{|U|}{4} + o(|U|^2). \quad (\text{A.6})$$

Thus, the QP eigenstates take the simple form $|\Psi_\pm\rangle = \frac{1}{\sqrt{2}} (|\Psi_2^0\rangle \pm |\Psi_3^0\rangle)$, their respective energy being $E_\pm = \mp \frac{1}{4}|U|$.

Using the expressions of $|\phi_0^\pm\rangle$ as given in Eq.(A.3), one finds, $\langle c_{Ak,\uparrow}^\dagger c_{Ak,\uparrow} \rangle = \langle c_{Ak,\uparrow}^\dagger c_{Ak,\downarrow}^\dagger \rangle = \frac{1}{4}(1 + \sin(k))$. After a trivial Fourier transform, we finally end up with,

$$G_{AA}(r) = K_{AA}(r) = \frac{1}{4}\delta_{r,0} - \frac{i}{8}\delta_{r,a} + \frac{i}{8}\delta_{r,-a}. \quad (\text{A.7})$$

In addition for the off-diagonal CFs it is found that,

$$G_{AB}(r) = K_{AB}(r) = \frac{1}{8}(\delta_{r,a} + \delta_{r,-a}). \quad (\text{A.8})$$

These results explain the data plotted in Fig. 5 of the present manuscript. We recall that our proof is restricted to $|U| \leq t$.

APPENDIX B : THE CORRELATION FUNCTIONS IN THE χ -LATTICE

In this appendix, our purpose is to derive analytically the correlation functions G and K in the quarter filled χ -Lattice. The BdG calculations are performed for small values of the Hubbard parameter $|U|$ at $T = 0$ K. The BdG Hamiltonian has the same form as that given in Eq.(A.1) of the Appendix A, with \hat{h}_k^\uparrow now given by,

$$\hat{h}_k^\uparrow = \begin{pmatrix} -\mu - \frac{|U|}{4}n & -te^{-i\alpha_k} \\ -te^{i\alpha_k} & -\mu - \frac{|U|}{4}n \end{pmatrix}, \quad (\text{B.1})$$

where $\alpha_k = \chi(\cos(k_x a) + \cos(k_y a))$.

Notice that the χ -Lattice is both bipartite and time reversal symmetric as well which implies $\hat{h}_k^{\downarrow*} = \hat{h}_k^\uparrow$.

To calculate the QP eigenstates, we use the same notation as those of Appendix A. At $|U| = 0$, the quasi-particle (QP) eigenstates are located at $E_{1,4} = \pm 2t$, and $E_{2,3} = 0$ which is doubly degenerate, the chemical potential being $\mu = \mu_0 = -t$. The one particle eigenstates read,

$$|\phi_0^\pm\rangle = \frac{1}{\sqrt{2}} \begin{pmatrix} \mp e^{-i\frac{\alpha_k}{2}} \\ e^{i\frac{\alpha_k}{2}} \end{pmatrix}. \quad (\text{B.2})$$

The equations (A.4), (A.5) and (A.6) of Appendix A are valid as well in the case of the $\chi - L$ at quarter filling. Thus one straightforwardly gets, $\langle \hat{c}_{Ak,\uparrow}^\dagger \hat{c}_{Ak,\uparrow} \rangle = \frac{1}{4}$, $\langle \hat{c}_{Ak,\uparrow}^\dagger \hat{c}_{Bk,\uparrow} \rangle = \frac{1}{4}e^{-i\alpha_k}$, $\langle \hat{c}_{Ak,\uparrow}^\dagger \hat{c}_{A-k,\downarrow}^\dagger \rangle = \frac{1}{4}$ and $\langle \hat{c}_{Ak,\uparrow}^\dagger \hat{c}_{B-k,\downarrow}^\dagger \rangle = \frac{1}{4}e^{-i\alpha_k}$. It follows that,

$$G_{AA}(\mathbf{r}) = K_{AA}(\mathbf{r}) = \frac{1}{4}\delta_{\mathbf{r},0}, \quad (\text{B.3})$$

and the off-diagonal CFs are,

$$G_{AB}(\mathbf{r}) = K_{AB}(\mathbf{r}) = \frac{1}{4}f_{AB}(\mathbf{r}), \quad (\text{B.4})$$

where, we have introduced $f_{AB}(\mathbf{r}) = \frac{1}{N_c} \sum_{\mathbf{k}} e^{i\mathbf{k}\cdot\mathbf{r}} e^{-i\alpha_{\mathbf{k}}}$. Thus, $G_{AB}(\mathbf{r})$ and $K_{AB}(\mathbf{r})$ coincide, up to a constant, with the (A,B) hoppings. We now propose to calculate the analytic expression of $f_{AB}(\mathbf{r})$ for both $|\mathbf{r}|/a \leq \chi$ and $|\mathbf{r}|/a \gg \chi$.

Let us write $\mathbf{r} = (n_x, n_y)$, $f_{AB}(\mathbf{r})$ can be rewritten as the following product,

$$f_{AB}(\mathbf{r}) = I_{n_x}(-i\chi) \cdot I_{n_y}(-i\chi), \quad (\text{B.5})$$

where $I_n(i\chi) = \frac{1}{2\pi} \int_{-\pi}^{+\pi} e^{in\theta} e^{i\chi \cos(\theta)}$ is the modified Bessel function of the first kind and order n . We can now rely on the properties of the Bessel functions such as $I_n(-i\chi) = (-i)^n J_n(\chi)$ which leads to,

$$f_{AB}(\mathbf{r}) = (-i)^{n_x+n_y} J_{n_x}(\chi) \cdot J_{n_y}(\chi). \quad (\text{B.6})$$

In the regime where $|\mathbf{r}| \leq \chi a$ one can expand the Bessel function [42],

$$J_n(\chi) \simeq \sqrt{\frac{2}{\pi\chi}} \cos\left(\chi - n\frac{\pi}{2} - \frac{\pi}{4}\right), \quad (\text{B.7})$$

and similarly for $J_m(\chi)$. This clearly explains the presence of the oscillations observed in Fig. 6 of the manuscript.

In the opposite limit, more precisely for $\chi \ll \sqrt{|n_x| + |n_y|}$, one has,

$$J_n(\chi) \simeq \frac{1}{\Gamma(n+1)} \left(\frac{\chi}{2}\right)^n. \quad (\text{B.8})$$

According to the well known Stirling formula, for $n \gg 1$ one can write $\Gamma(n+1) \simeq \frac{1}{\sqrt{2\pi n}} \left(\frac{n}{e}\right)^n$. Thus, along the x -direction for instance, it implies the following result,

$$f_{AB}(\mathbf{r}) = (-i)^{n_x} \frac{J_0(\chi)}{\sqrt{2\pi n_x}} e^{n_x \ln\left(\frac{e\chi}{2n_x}\right)}. \quad (\text{B.9})$$

This equation explains (i) the rapid decay observed in Fig. 6 of our manuscript and (ii) the impossibility to extract a characteristic lengthscale from the decay at large distance of the off-diagonal correlation functions.

* maxime.thumin@neel.cnrs.fr

† georges.bouzerar@neel.cnrs.fr

- [1] Daniel Leykam, A. & Flach, S. Artificial flat band systems : from lattice models to experiments. *Advances In Physics : X.* **3**, 1473052 (2018), <https://doi.org/10.1080/23746149.2018.1473052>
- [2] Regnault, N., Xu, Y., Li, M., Ma, D., Jovanovic, M., Yazdani, A., Parkin, S., Felsner, C., Schoop, L., Ong, N., Cava, R., Elcoro, L., Song, Z. & Bernevig, B. Catalogue of flat-band stoichiometric materials. *Nature.* **603**, 824-828 (2022,3), <https://doi.org/10.1038/s41586-022-04519-1>

- [3] Tang, L., Song, D., Xia, S., Xia, S., Ma, J., Yan, W., Hu, Y., Xu, J., Leykam, D. & Chen, Z. . *Nanophotonics.* **9**, 1161-1176 (2020), <https://doi.org/10.1515/nanoph-2020-0043>
- [4] Poblete, R. Photonic flat band dynamics. *Advances In Physics : X.* **6**, 1878057 (2021), <https://doi.org/10.1080/23746149.2021.1878057>
- [5] BERGHOLTZ, E. & LIU, Z. TOPOLOGICAL FLAT BAND MODELS AND FRACTIONAL CHERN INSULATORS. *International Journal Of Modern Physics B.* **27**, 1330017 (2013), <https://doi.org/10.1142/S021797921330017X>
- [6] Rhim, J. & Yang, B. Singular flat bands. *Advances In Physics : X.* **6**, 1901606 (2021), <https://doi.org/10.1080/23746149.2021.1901606>
- [7] Derzhko, O., Richter, J. & Maksymenko, M. Strongly correlated flat-band systems : The route from Heisenberg spins to Hubbard electrons. *International Journal Of Modern Physics B.* **29**, 1530007 (2015), <https://doi.org/10.1142/S0217979215300078>
- [8] Balents, L., Dean, C., Efetov, D. & Young, A. Superconductivity and strong correlations in moiré flat bands. *Nature Physics.* **16**, 725-733 (2020,7), <https://doi.org/10.1038/s41567-020-0906-9>
- [9] Kopnin, N., Heikkilä, T. & Volovik, G. High-temperature surface superconductivity in topological flat-band systems. *Phys. Rev. B.* **83**, 220503 (2011,6), <https://link.aps.org/doi/10.1103/PhysRevB.83.220503>
- [10] Heikkilä, T., Kopnin, N. & Volovik, G. Flat bands in topological media. *JETP Letters.* **94**, 233-239 (2011,10), <https://doi.org/10.1134/S0021364011150045>
- [11] Peotta, S. & Törmä, P. Superfluidity in topologically nontrivial flat bands. *Nature Communications.* **6**, 8944 (2015,11), <https://doi.org/10.1038/ncomms9944>
- [12] Mondaini, R., Batrouni, G. & Grémaud, B. Pairing and superconductivity in the flat band : Creutz lattice. *Phys. Rev. B.* **98**, 155142 (2018,10), <https://link.aps.org/doi/10.1103/PhysRevB.98.155142>
- [13] Huhtinen, K., Herzog-Arbeitman, J., Chew, A., Bernevig, B. & Törmä, P. Revisiting flat band superconductivity : Dependence on minimal quantum metric and band touchings. *Phys. Rev. B.* **106**, 014518 (2022,7), <https://link.aps.org/doi/10.1103/PhysRevB.106.014518>
- [14] Chan, S., Grémaud, B. & Batrouni, G. Designer flat bands : Topology and enhancement of superconductivity. *Phys. Rev. B.* **106**, 104514 (2022,9), <https://link.aps.org/doi/10.1103/PhysRevB.106.104514>
- [15] Liang, L., Vanhala, T., Peotta, S., Siro, T., Harju, A. & Törmä, P. Band geometry, Berry curvature, and superfluid weight. *Phys. Rev. B.* **95**, 024515 (2017,1), <https://link.aps.org/doi/10.1103/PhysRevB.95.024515>
- [16] Hofmann, J., Berg, E. & Chowdhury, D. Superconductivity, pseudogap, and phase separation in topological flat bands. *Phys. Rev. B.* **102**, 201112 (2020,11), <https://link.aps.org/doi/10.1103/PhysRevB.102.201112>
- [17] Iskin, M. Origin of flat-band superfluidity on the Mielke checkerboard lattice. *Phys. Rev. A.* **99**, 053608 (2019,5), <https://link.aps.org/doi/10.1103/PhysRevA.99.053608>
- [18] Thumin, M. & Bouzerar, G. Constraint relations for superfluid weight and pairings in a chiral flat band superconductor. *Europhysics Letters.* **144**, 56001 (2023,12), <https://dx.doi.org/10.1209/0295-5075/ad0dc6>
- [19] Provost, J. & Vaille, G. Riemannian structure on manifolds of quantum states. *Communications*

- In *Mathematical Physics*. **76**, 289-301 (1980,9), <https://doi.org/10.1007/BF02193559>
- [20] Resta, R. The insulating state of matter : a geometrical theory. *The European Physical Journal B*. **79**, 121-137 (2011,1), <https://doi.org/10.1140/epjb/e2010-10874-4>
- [21] Cao, Y., Fatemi, V., Fang, S., Watanabe, K., Taniguchi, T., Kaxiras, E. & Jarillo-Herrero, P. Unconventional superconductivity in magic-angle graphene superlattices. *Nature*. **556**, 43-50 (2018,4), <https://doi.org/10.1038/nature26160>
- [22] Cao, Y., Fatemi, V., Demir, A., Fang, S., Tomarken, S., Luo, J., Sanchez-Yamagishi, J., Watanabe, K., Taniguchi, T., Kaxiras, E., Ashoori, R. & Jarillo-Herrero, P. Correlated insulator behaviour at half-filling in magic-angle graphene superlattices. *Nature*. **556**, 80-84 (2018,4), <https://doi.org/10.1038/nature26154>
- [23] Park, J., Cao, Y., Watanabe, K., Taniguchi, T. & Jarillo-Herrero, P. Tunable strongly coupled superconductivity in magic-angle twisted trilayer graphene. *Nature*. **590**, 249-255 (2021,2), <https://doi.org/10.1038/s41586-021-03192-0>
- [24] Zhang, X., Tsai, K., Zhu, Z., Ren, W., Luo, Y., Carr, S., Luskin, M., Kaxiras, E. & Wang, K. Correlated Insulating States and Transport Signature of Superconductivity in Twisted Trilayer Graphene Superlattices. *Phys. Rev. Lett.* **127**, 166802 (2021,10), <https://link.aps.org/doi/10.1103/PhysRevLett.127.166802>
- [25] Bistritzer, R. & Allan H. MacDonald Moiré bands in twisted double-layer graphene. *Proceedings Of The National Academy Of Sciences*. **108**, 060505 (2011)
- [26] Julku, A., Peltonen, T., Liang, L., Heikkilä, T. & Törmä, P. Superfluid weight and Berezinskii-Kosterlitz-Thouless transition temperature of twisted bilayer graphene. *Phys. Rev. B*. **101**, 060505 (2020,2), <https://link.aps.org/doi/10.1103/PhysRevB.101.060505>
- [27] Bardeen, J., Cooper, L. & Schrieffer, J. Theory of Superconductivity. *Phys. Rev.* **108**, 1175-1204 (1957,12), <https://link.aps.org/doi/10.1103/PhysRev.108.1175>
- [28] Tinkham, M. *Introduction to Superconductivity*. (Dover Publications,2004)
- [29] Pitaevskii, L. & Stringari, S. *Bose-Einstein Condensation*. (Oxford University Press,2003)
- [30] Leggett, A. *Quantum Liquids : Bose Condensation and Cooper Pairing in Condensed-Matter Systems*. (Oxford University Press,2006)
- [31] Chen, S. & Law, K. Ginzburg-Landau Theory of Flat-Band Superconductors with Quantum Metric. *Phys. Rev. Lett.* **132**, 026002 (2024,1), <https://link.aps.org/doi/10.1103/PhysRevLett.132.026002>
- [32] Hu, J., Chen, S. & Law, K. Anomalous Coherence Length in Superconductors with Quantum Metric. (2023)
- [33] Hofmann, J., Chowdhury, D., Kivelson, S. & Berg, E. Heuristic bounds on superconductivity and how to exceed them. *Npj Quantum Materials*. **7**, 83 (2022,8), <https://doi.org/10.1038/s41535-022-00491-1>
- [34] Hofmann, J., Berg, E. & Chowdhury, D. Superconductivity, Charge Density Wave, and Superfluidity in Flat Bands with a Tunable Quantum Metric. *Phys. Rev. Lett.* **130**, 226001 (2023,5), <https://link.aps.org/doi/10.1103/PhysRevLett.130.226001>
- [35] Berezinsky, V. Destruction of Long-range Order in One-dimensional and Two-dimensional Systems Possessing a Continuous Symmetry Group. II. Quantum Systems.. *Sov. Phys. JETP*. **34**, 610 (1972)
- [36] Kosterlitz, J. & Thouless, D. Long range order and metastability in two dimensional solids and superfluids. (Application of dislocation theory). *Journal Of Physics C : Solid State Physics*. **5**, L124 (1972,6), <https://dx.doi.org/10.1088/0022-3719/5/11/002>
- [37] Kosterlitz, J. & Thouless, D. Ordering, metastability and phase transitions in two-dimensional systems. *Journal Of Physics C : Solid State Physics*. **6**, 1181 (1973,4), <https://dx.doi.org/10.1088/0022-3719/6/7/010>
- [38] Chan, S., Grémaud, B. & Batrouni, G. Pairing and superconductivity in quasi-one-dimensional flat-band systems : Creutz and sawtooth lattices. *Phys. Rev. B*. **105**, 024502 (2022,1), <https://link.aps.org/doi/10.1103/PhysRevB.105.024502>
- [39] Bouzerar, G. & Thumin, M. Hidden symmetry of Bogoliubov de Gennes quasi-particle eigenstates and universal relations in flat band superconducting bipartite lattices. *SciPost Phys. Core*. **7** pp. 018 (2024), <https://scipost.org/10.21468/SciPostPhysCore.7.2.018>
- [40] Bouzerar, G. Giant boost of the quantum metric in disordered one-dimensional flat-band systems. *Phys. Rev. B*. **106**, 125125 (2022,9), <https://link.aps.org/doi/10.1103/PhysRevB.106.125125>
- [41] Thumin, M. & Bouzerar, G. Flat-band superconductivity in a system with a tunable quantum metric : The stub lattice. *Phys. Rev. B*. **107**, 214508 (2023,6), <https://link.aps.org/doi/10.1103/PhysRevB.107.214508>
- [42] Watson, G. *A Treatise on the Theory of Bessel Functions*. (Cambridge University Press,1995), <https://books.google.ca/books?id=MLk3FrNoEV0C>